ARTICLES

Journal of Semiconductors
(2019) 40, 012805
doi: 10.1088/1674-4926/40/1/012805

Current transport mechanism of Mg/Au ohmic contacts to lightly doped n-type β-Ga_2O_3

Jianjun Shi, Xiaochuan Xia, Qasim Abbas, Jun Liu, Heqiu Zhang, Yang Liu, and Hongwei Liang[†]

School of Microelectronics, Dalian University of Technology, Dalian 116024, China

Abstract: The carrier transport mechanism of Mg/Au ohmic contact for lightly doped β-Ga_2O_3 is investigated. An excellent ohmic contact has been achieved when the sample was annealed at 400 °C and the specific contact resistance is 4.3×10^{-4} Ω·cm². For the annealed sample, the temperature dependence of specific contact resistance is studied in the range from 300 to 375 K. The specific contact resistance is decreased from 4.3×10^{-4} to 1.59×10^{-4} Ω·cm² with an increase of test temperature. As combination with the judge of E_{00}, the basic mechanism of current transport is dominant by thermionic emission theory. The effective barrier height between Mg/Au and β-Ga_2O_3 is evaluated to be 0.1 eV for annealed sample by fitting experimental data with thermionic emission model.

Key words: Mg/Au; beta-gallium oxide; ohmic contact; thermionic emission theory; effective barrier height

Citation: J J Shi, X C Xia, Q Abbas, J Liu, H Q Zhang, Y Liu, and H W Liang, Current transport mechanism of Mg/Au ohmic contacts to lightly doped n-type β-Ga_2O_3[J]. *J. Semicond.*, 2019, 40(1), 012805. http://doi.org/10.1088/1674-4926/40/1/012805

1. Introduction

Beta gallium oxide (β-Ga_2O_3), with a large band gap of about 4.8 eV and a high theoretical breakdown electric field of 8 MV/cm[1, 2], has gained prominent attention to be applied as an adequate material for high power electronic devices. The Baliga's figure of merit for β-Ga_2O_3 is about ten times larger than that of 4H-SiC and four times larger than that of GaN[3]. Another important advantage of β-Ga_2O_3 is that larger-area single-crystal substrates can be synthesized by several conventional melt growth methods, commonly employed are Czochralski (CZ)[4, 5], floating-zone (FZ)[6, 7], and edge-defined film-fed growth (EFG)[8–10]. In addition, carrier concentration of n-type β-Ga_2O_3 can be controlled by doping with Sn/Si in range of 10^{15}–10^{19} cm^{-3}[11, 12].

The metal oxide semiconductor field-effect transistors (MOSFET) and schottky barrier diodes are two critical power electronics application of β-Ga_2O_3. Low resistance ohmic contacts are essential for β-Ga_2O_3 devices to reduce devices' conduction loss. Several groups[13–15] have employed heavily doping by ion implantation technique and an intermediate semiconductor layer between metal and semiconductor to form ohmic contact. However, both of them were either expensive or complex. Additionally, in spite of the resistance of ohmic contacts per unit area being as low as 4.6×10^{-6} Ω·cm², the mechanism of current transport in β-Ga_2O_3 ohmic contacts has received a little attention and is reported rarely. The current transport mechanism is vital for improving performance of β-Ga_2O_3-based powder devices to understand the basic electrical characteristic of ohmic contact on β-Ga_2O_3 surface, including Schottky barrier height and the carrier transport mechanism.

Up till now, four leading model of current flow in the metal–semiconductor ohmic contact are developed, namely, the thermionic emission theory (TE), field emission (FE), thermal-field emission theory (TFE), and metallic shunts model[16]. The E_{00} is defined as $qh/4\pi[N/(m^*\varepsilon_s)]^{1/2}$. Here, h is the Plank constant, N is carrier concentration in the semiconductor, ε_s is the permittivity of the semiconductor, q is the elementary charge, and m^* is the effective mass of electron in the semiconductor. (Ⅰ) For thermionic emission theory, $\rho_c T \propto \exp\left(\frac{q\varphi_b}{kT}\right)$, the specific contact resistance (ρ_c) of the ohmic contact decreases with increasing temperature and rises exponentially with an increase in φ_b between metal and semiconductor. Here, k is Boltzmann constant and φ_b is the effect barrier height between metal and semiconductor. (Ⅱ) For field emission theory, $\rho_c \propto \exp\left(\frac{\varphi_b}{E_{00}}\right)$, ρ_C increases with φ_b and decrease with increasing carrier concentration of uncompensated impurities in a semiconductor, and is virtually independent of the temperature. (Ⅲ) For thermal-field emission theory, $\rho_c \propto \exp\left(\frac{\varphi_b}{E_{00}\coth(qE_{00}/kT)}\right)_b$, ρ_c should increase with an increase in φ_b and weakly decreases with an increase of temperature. (Ⅳ) For metallic shunts model, ρ_C increases with temperature. In addition, there is another criterion for judging in which current transport model is dominant: when $qE_{00}/kT < 0.5$, the thermal emission mechanism is dominant; when $qE_{00}/kT > 5$, the field emission is dominant; when $0.5 < qE_{00}/kT < 5$, the thermionic field emission is dominant.

In this letter, Mg/Au is used to prepare ohmic contact with lightly doped β-Ga_2O_3 because of its low work function, high humidity resistance, oxygen resistance, and corrosion resistance[17, 18]. The Mg/Au stacks exhibit excellent ohmic contact properties on lightly doped β-Ga_2O_3 after annealing at 400 °C. To investigate current transport mechanism on β-Ga_2O_3, the dependence of current–voltage on measuring temperature was performed, followed by an analysis based on TE

Correspondence to: H W Liang, hwliang@dlut.edu.cn
Received 3 AUGUST 2018; Revised 5 OCTOBER 2018.

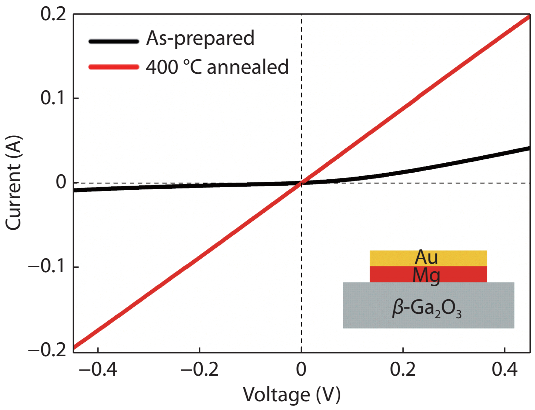

Fig. 1. (Color online) I–V curves for as-prepared and 400 °C annealed samples. The insert is the schematic structure of the Mg/Au/β-Ga_2O_3 contact.

model.

2. Experimental

The Sn lightly doped ($\bar{2}01$)-oriented β-Ga_2O_3 substrate with 680 μm thickness was used by cutting into 5 × 5 mm^2 pieces. The carrier concentration of single crystal β-Ga_2O_3 substrate was about 4.94 × 10^{17} cm^{-3}. Prior to metal deposition, the substrate was cleaned in methanol, acetone, methanol, and deionized water (DIW) by ultra-sonication for 5 minutes, respectively. Next, the substrates were dipped in Piranha solutions (DIW (30 %) : H_2O_2 (96%) : H_2SO_4 = 1 : 1 : 4) solution for 5 min. Then, the substrates were dipped in DIW at 90 °C for 5 min, later cooled down to room temperature. Finally, the substrate was rinsed in HF (> 40%) for 5 h. Metal deposition was performed by conventional thermal evaporation method. The Mg metal (99.999%) was evaporated with the thickness of 820 nm, followed by 600 nm thick Au metal film coating. Then metal electrodes were annealed at an optimum temperature of 400 °C for 2 min in a quartz tube under Ar gas protection. The contact metal pads for transmission line method (TLM) testers were formed by standard lithography process with space of 0.15, 0.2, 0.25, 0.3, and 0.4 mm. The dimensions of contact metal pads are 0.4 × 1.2 mm^2.

The current–voltage characteristics were measured using Keithley 2611A semiconductor characterization system in the range of 300–375 K. The ρ_c was extracted using the transmission line method (TLM). Hall Effect 5500 PC measurement system was employed to determine the carrier concentration of bulk β-Ga_2O_3.

3. Results and discussion

Fig. 1 shows the current–voltage characteristics of as-deposited and annealed Mg/Au/β-Ga_2O_3 contacts samples, as measured from adjacent contact pads with a gap spacing of 0.15 mm. For the as-prepared sample, the I–V curves showed nonlinear behavior, while sample annealed at 400 °C showed the linear behavior of current–voltage curve, which indicates that thermal annealing can lead to the formation of ohmic contacts.

Suzuki *et al.*[19] reported that the barrier height of Au/β-Ga_2O_3 contact decreased with an increase in the annealing temperature. Similarly, in our experiment, the annealing results in lowing the barrier height between Mg/Au and β-Ga_2O_3 interfaces and formed ohmic contact to show linear I–V characteristic.

Fig. 2(a) shows the dependence of the experimentally measured total resistance (R_T) on distance (d) between two adjacent contact pads for the annealed sample at different measuring temperatures. The R_T can be represented by equation:

$$R_T = 2R_C + \frac{dR_{SH}}{W} = 2R_C + \frac{d}{qN\mu_n S}.$$

Here, R_C and R_{SH} are contact resistance and sheet resistance, respectively. The d, W, q, N, μ_n and S are the distance of adjacent electrodes, width of electrodes, element charge, carrier concentration, carrier mobility and electrode area, respectively. The intercept of line with the ordinate axis corresponds to double R_C and its slope is proportional to the R_{SH}. The dependence of R_T on d is linear at each measuring temperature, as shown in Fig. 2(a). Fig. 2(b) shows that the R_C decreases from 0.96 to 0.8 Ω and R_{SH} increases from 0.3 to 0.56 Ω/□ as measuring temperature rise from 300 to 375 K. As we know, the carrier mobility is affected by temperature and it decrease with increasing measuring temperature at high temperature. Thus, the reason of the increase of R_{SH} with increasing the testing temperature could be attributed to the decrease of electron mobility.

In order to investigate the current transport mechanism of Mg/Au ohmic contact for annealed sample, the ρ_c was extracted as a function of measuring temperature. The ρ_c decreased slightly from 4.3 × 10^{-4} to 1.59 × 10^{-4} Ω·cm^2 in the measuring temperature range from 300 to 375 K, as shown in Fig. 3. According the model of current flow in the metal semiconductor ohmic contact, TFE and FE model may be the basic theories of current transport at the Mg/Au-β-Ga_2O_3 ohmic contact interface. However, judging from E_{00}, it is calculated to be 0.007 V and qE_{00}/kT (T = 300 K) is 0.27 < 0.5. Where, the m^* is 0.28m_e[20], ε_S is 10 for β-Ga_2O_3, with N is 4.94 × 10^{17} cm^{-3} measured by Hall Effect 5500 PC measurement system. Consideration with the lightly doped β-Ga_2O_3, it is reasonable to conclude that the mechanism of current transport is dominated by thermionic emission theory in the present system rather than thermal-field emission theory.

For FE theory, $\rho_c T \propto \exp\left(\frac{q\varphi_b}{kT}\right)$, the dependence of $\rho_c T$ on $1/T$ should be linear on a semi-logarithmic scale with the slope of this dependence proportional to the barrier height φ_b. Fig. 4 gives the experimental and theoretical relationships between $\rho_c T$ and $1/T$. It is fitted well between them, which means that the current transport mechanism of Mg/Au/β-Ga_2O_3 ohmic contact is FE consistent with the previous discussion. In addition, the effective barrier height is calculated to be 0.1 eV from the slope of the fitting curve. The effective barrier height between Mg/Au and β-Ga_2O_3 is sufficiently low which is responsible for the formation of the low contact resistance.

4. Conclusion

In summary, ohmic contact has been successfully realized on β-Ga_2O_3 using low work function Mg/Au stacks after annealing at 400 °C and the current transport mechanism was investigated. The temperature dependence of specific contact resistance of the Mg/Au-β-Ga_2O_3 ohmic contact decreased with increasing the measuring temperature from 300 to 375 K and qE_{00}/kT is 0.27 < 0.5. Therefore, the current transport mechan-

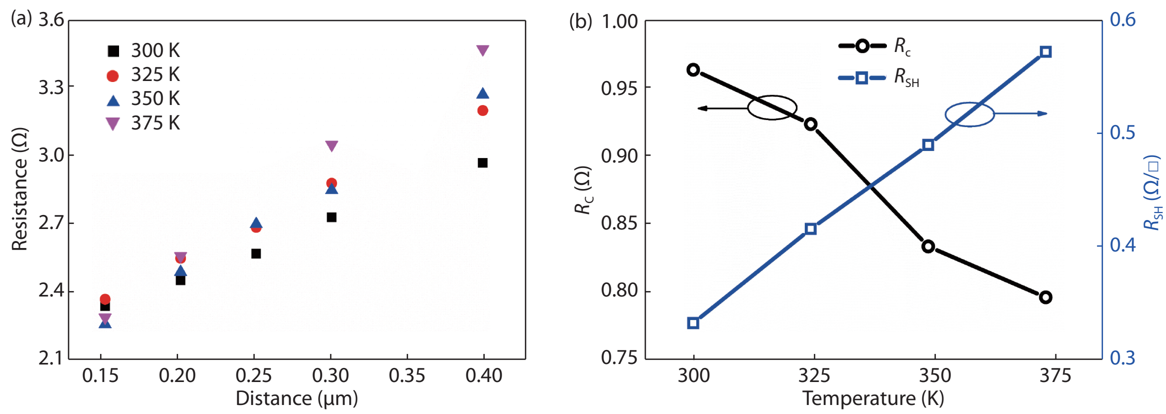

Fig. 2. (Color online) (a) Resistance of Mg/Au-β-Ga_2O_3 structure with two adjacent ohmic contacts versus the distance at different temperatures. (b) Contact resistance and sheet resistance of the ohmic contact Mg/Au-β-Ga_2O_3 versus measuring temperatures.

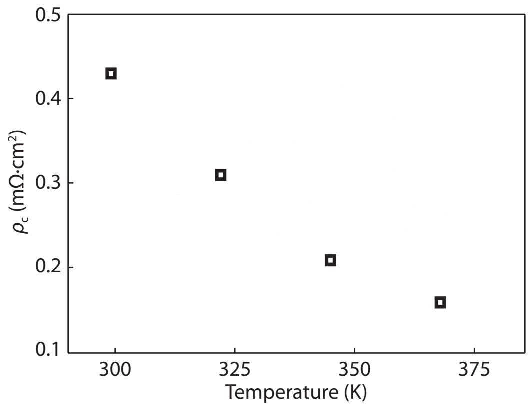

Fig. 3. (Color online) Specific contact resistance of the ohmic contact Mg/Au-β-Ga_2O_3 versus measuring temperatures.

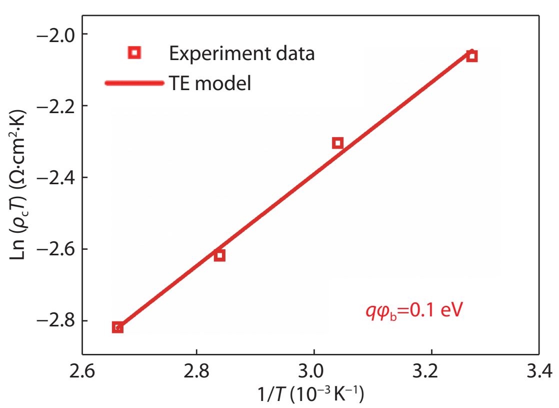

Fig. 4. (Color online) The dependence of ln ($\rho_c T$) on $1/T$ graph about Mg/Au-β-Ga_2O_3 ohmic contact for the annealed sample, experimental data (point) and TE model fitting (line).

ism is dominant thermionic emission theory. The effective barrier height extracted is 0.1 eV by fitting experiment data with thermionic emission model. Further investigation will be carried out on the heavily doped β-Ga_2O_3.

Acknowledgements

This work was supported by the National Key R&D Plan (Nos. 2016YFB0400600, 2016YFB0400601)，the National Science Foundation of China (Nos. 11675198, 61376046, 11405017, 61574026), the Fundamental Research Funds for the Central Universities (Nos. DUT15LK15, DUT15RC(3)016, No. DUT16LK29), the Liaoning Provincial Natural Science Foundation of China (Nos. 2014020004, 201602453, 201602176), the China Postdoctoral Science Foundation Funded Project (No. 2016M591434), the Open Fund of the State Key Laboratory on Integrated Optoelectronics (Nos. IOSKL2015KF18, IOSKL2015KF22).

References

[1] Chabak K, Green A, Moser N, et al. Gate-recessed, laterally-scaled beta-Ga_2O_3 MOSFETs with high-voltage enhancement-mode operation. 75th Annual Device Research Conference, 2017: 2

[2] Higashiwaki M, Sasaki K, Kuramata A, et al. Gallium oxide (Ga_2O_3) metal–semiconductor field-effect transistors on single-crystal β-Ga_2O_3 (010) substrates. Appl Phys Lett, 2012, 100(1), 013504

[3] Higashiwaki M, Sasaki K, Murakami H, et al. Recent progress in Ga_2O_3 power devices. Semicond Sci Technol, 2016, 31(3), 034001

[4] Irmscher K, Galazka Z, Pietsch M, et al. Electrical properties of β-Ga_2O_3 single crystals grown by the Czochralski method. J Appl Phys, 2011, 110(6), 063720

[5] Galazka Z, Uecker R, Irmscher K, et al. Czochralski growth and characterization of beta-Ga_2O_3 single crystals. Cryst Res Technol, 2010, 45(12), 1229

[6] Víllora E G, Shimamura K, Yoshikawa Y, et al. Large-size β-Ga_2O_3 single crystals and wafers. J Cryst Growth, 2004, 270(3/4), 420

[7] Ueda N, Hosono H, Waseda R, et al. Synthesis and control of conductivity of ultraviolet transmitting β-Ga_2O_3 single crystals. Appl Phys Lett, 1997, 70(26), 3561

[8] Kuramata A, Koshi K, Watanabe S, et al. High-quality beta-Ga_2O_3 single crystals grown by edge-defined film-fed growth. Jpn J Appl Phys, 2016, 55(12), 1202A

[9] Aida H., Nishiguchi K., Takeda H., et al Growth of beta-Ga_2O_3 single crystals by the edge-defined, film fed growth method. Jpn J Appl Phys, 2008, 47(11), 8506

[10] Mu W, Jia Z, Yin Y, et al. High quality crystal growth and anisotropic physical characterization of beta-Ga_2O_3 single crystals grown by EFG method. J Alloys Compnds, 2017, 714, 453

[11] Sasaki K, Kuramata A, Masui T, et al. Device-quality beta-Ga_2O_3 epitaxial films fabricated by ozone molecular beam epitaxy. Appl Phys Express, 2012, 5(3), 035502

[12] Víllora E G, Shimamura K, Yoshikawa Y, et al. Electrical conductivity and carrier concentration control in β-Ga_2O_3 by Si doping. Appl Phys Lett, 2008, 92(20), 202120

[13] Sasaki K, Higashiwaki M, Kuramata A, et al. Si-ion implantation doping in beta-Ga_2O_3 and its application to fabrication of low-resistance ohmic contacts. Appl Phys Express, 2013, 6(8), 086502

[14] Carey P H, Yang J, Ren F, et al. Ohmic contacts on n-type beta-

Ga_2O_3 using AZO/Ti/Au. AIP Adv, 2017, 7(9), 095313
[15] Carey P H, Jiancheng Y, Fan R, et al. Improvement of ohmic contacts on Ga_2O_3 through use of ITO-interlayers. J Vac Sci Technol B, 2017, 35(6), 061201
[16] Blank T V, Goldberg Y A, Posse E A. Flow of the current along metallic shunts in ohmic contacts to wide-gap III–V semiconductors. Semiconductors, 2009, 43(9), 1164
[17] Oyamada T, Sasabe H, Adachi C. Formation of MgAu alloy cathode by photolithography and its application to organic light-emitting diodes and organic field effect transistors. Electr Eng Jpn, 2005, 152(1), 37-42
[18] Arai H, Nakanotani H, Morimoto K, et al. Magnesium-gold binary alloy for organic light-emitting diodes with high corrosion resistance. J Vac Sci Technol B, 2016, 34(4), 040607
[19] Suzuki R, Nakagomi S, Kokubun Y, et al. Enhancement of responsivity in solar-blind β-Ga_2O_3 photodiodes with a Au Schottky contact fabricated on single crystal substrates by annealing. Appl Phys Lett, 2009, 94(22), 222102
[20] Knight S, Mock A, Korlacki R, et al. Electron effective mass in Sn-doped monoclinic single crystal beta-gallium oxide determined by mid-infrared optical Hall effect. Appl Phys Lett, 2018, 112(1), 012103